Extinction Mechanism of a Diffusion Flame at Low or High Stretch Rate

Shangqing Tao, Jun Fang*, Lizhong Yang
University of Science and Technology of China, State Key Laboratory of Fire Science, Hefei, Anhui, P. R. China

Abstract

Extremely high stretch rate can cause flame extinction which has been widely investigated. The buoyant flow around a flame on Earth precludes studying the effect of low stretch rate on flames. While low stretch rate is common in low-gravity environments and can also cause flame extinction. This study aims to fill the void in flame suppuration by low stretch rate and also to provide insight for microgravity and extraterrestrial fire safety applications. Extinction mode with a 'U'-shape flammability map was found and two different mechanisms were proposed: "quenching" corresponding to low stretch rate which is similar to extinction of microgravity flames, and "blowoff" corresponding to high stretch rate which is usually found in highly forced flow environment. Furthermore, ice bath was employed to inquiry the effect of heat loss. The important chemical kinetic parameter Damkohler number (*Da*) was analyzed, where quenching branch corresponds to radiative extinction state ($Da_{E,R}$) and blowoff branch corresponds to the kinetic extinction state ($Da_{E,K}$). This study is instructive for extinction of fires.

Keywords: Quenching, Blowoff, Varied stretch rate, Flammability map**,** Damkohler number.

Introduction

Stretch rate can be interpreted as inducing by the tangential gradient of the flow velocity or the flame curvature over the flame surface where it is evaluated [1]. Thus, stretched flames are commonly seen in a real fire scene. Furthermore, extreme stretch rates are often related to flame suppression and extinction. Karlovitz et al. [2] first introduced the concept of flame stretch as a means of evaluating the extinction and stabilization of premixed turbulent flames. Subsequently, the concept has been successfully extended to the study of diffusion flames.

Researches about flame suppression under effect of stretch are mostly for cases of high stretch rate. This is because highly stretched flame can be gained more easily in an earth-based environment including the effect of buoyancy and can become extinguished. Clearly at extinction, chemical kinetic effects become important so that flame stretch is often incorporated into a non-dimensional chemical and physical factor *Da*, which is a measure between chemical reaction time to flow residence time in the flame and expressed as [3]:

$$Da = \frac{t_{Diff}}{t_{chem}} \sim \frac{\text{reaction rate}}{\text{flow rate}} = \frac{B}{a} \qquad \text{(Eq. 1)}$$

Where *B* is the pre-exponential factor of the reaction and *a* is the stretch rate. Based on a previous theoretical study [4], an earth equivalent stretch rate induced by buoyancy (a_b) is:

$$a_b = \left(\frac{T^* - T_\infty}{T^*} \frac{g}{R} \right)^{1/2} \qquad \text{(Eq. 2)}$$

Where T^* is the reference flame temperature, T_∞ is the ambient temperature, *g* is the acceleration of gravity, *R* is the sample radius. It indicates that varied stretch rates can be obtained by changing *R*.

Purely forced flow induced stretch rate (a_f) can be written as the tangential gradient of the flow velocity [4]:

$$a_f = \begin{cases} 2U/R & (\text{for cylinder}) \\ 3U/2R & (\text{for sphere}) \end{cases} \qquad \text{(Eq. 3)}$$

Stretch rate in the mixed convective environment is [4]:

$$a = \left(a_b^2 + a_f^2 \right)^{1/2} \qquad \text{(Eq. 4)}$$

At very high stretch rate, *Da* becomes small, the small flow diffusion time compared to chemical reaction time causes dropped flame temperature, and eventually these effects of excessive stretch lead to flame extinction. This kind of extinction is called “blowoff” and has been widely discussed in the past. For most flames on Earth, the buoyant flow around a flame precludes studying the effect of low stretch rates on flames. Diffusion flames at very low stretch rate, however, would be common in low-gravity environments and may also lead to flame extinction.

Therefore, the motivation of this study is to provide a comprehensive understanding of suppression and extinction under effects of high or low stretch rate as well as reduced oxygen concentration in a terrestrial environment.

Experimental setup and methodology

Fig. 1 shows a stagnation-point configuration setup which can provide a range of stretch rates by varying PMMA sample radius. The oxygen concentration is adjusted by two flows of nitrogen and air using two mass flow controllers. The gas mixture exits from a honeycomb which can straighten the flow to the base of the curved PMMA sample.

Samples used in this experiment were cut from the same batch of PMMA. For larger radii samples (*R*=20, 50, 75, 100, 200 cm), 30 cm×30 cm×2.5 cm dimension slabs were first cut and then pre-heated at 160 °C until pliable. These pliable slabs were immediately placed between two curved molds made of steel plates having the desired radius of curvature. Then, they were allowed to cool to room temperature to permit stress relaxation. Finally, PMMA samples with different radius of curvature were obtained. While radii of 2.5 and 5 cm samples were obtained by halving the whole size cylinders.

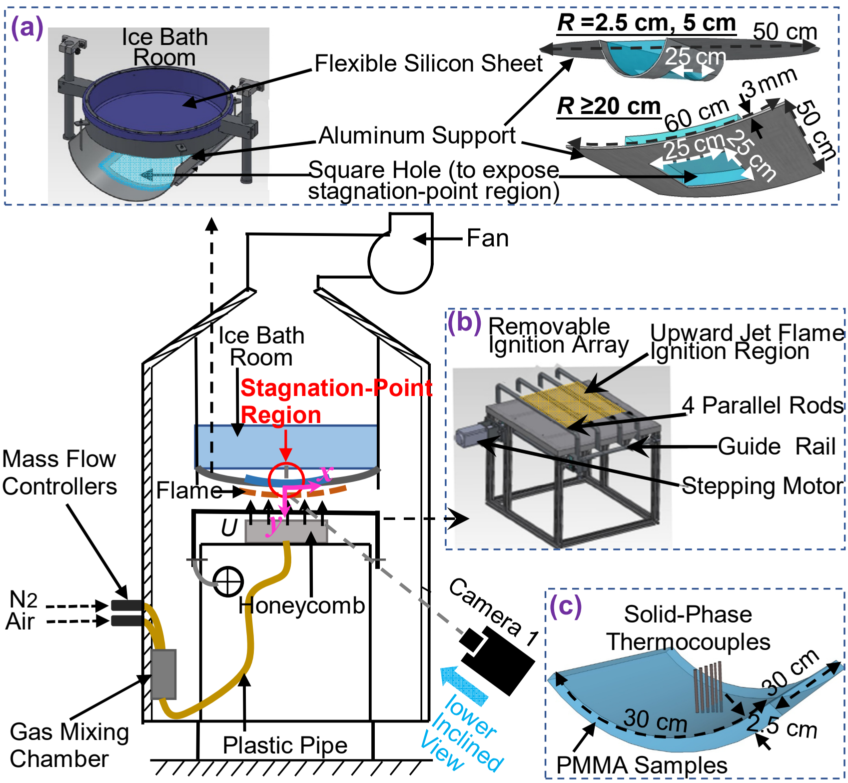

Fig. 1. Experimental setup (a: Ice bath and aluminum support connection; b: Removable ignition array; c: Solid-phase thermocouples.).

Aluminum supports with a size of $50\ \mathrm{cm} \times 60\ \mathrm{cm} \times 3\ \mathrm{mm}$ have the same curvature with their connected samples, as shown in Fig. 1a. In the case of *R*≥20 cm, a $25\ \mathrm{cm} \times 25\ \mathrm{cm}$ square hole was pre-cut in the center of each support to expose the stagnation-point region of the sample. In this geometry, there was one diffusion flame configuration where only stagnation-point flame zone existed [3]. Basically, all the scalar quantities (temperature and species concentrations) were (quasi-) one-dimensional in the *x* direction. While for *R*=2.5, 5 cm, it was impossible to cut the same size hole, so half-cylindrical aluminum sheets were used to support these samples, with smaller holes in the center.

Right above the curved PMMA sample, there was an ice bath room to which a 0.5 mm flexible silicon sheet was fixed, to let the ice/water mixture cover the upper surface of the sample. Half of the tests employed ice bath to make clear of the effects of solid in-depth heat loss.

As seen in Fig. 1b, the complete ignition of the exposed sample surface was achieved by using an igniter array comprising 4 parallel rods with small, evenly spaced pores. An array of upward jet propane flames was formed at these pores, covering an area a little larger than the exposed sample surface. The igniter array was positioned between the sample base and the honeycomb. After ignition, it was removed to one side by a stepping motor to avoid the disturbance in the flow under the sample. The extinction process was recorded by a video camera (Camera 1, Sony AX60) from the lower inclined view.

Six K-type thermocouples with 0.1 cm outer diameter wires (±2 °C) were placed along the direction of the sample axis near its center to record the solid-phase temperature. Four of these thermocouples were embedded at four different depths with evenly space in the sample, while one of the remaining two was attached to the base and the other to the top surface, as seen in the Fig. 1c.

The oxygen concentration in the gap between the honeycomb and the sample base was measured according to a high temperature probe (TESTO 340, resolution: 0.1 %). Similar to the method used by Johnston and T'ien [5], during each test of a fixed sample radius, the oxygen concentration was reduced in steps of about 1 % at 100 s intervals after pseudo-steady combustion was achieved. Eventually, the flame was extinguished to get the limited oxygen concentration. Each test was repeated at least three times to eliminate random errors.

Extinction behavior of stretched flame

Figure 2 captures sequential images from local to total extinction with reduced oxygen concentration for *R*=100 cm with ice bath. Fig. 2a demonstrates the low inclined viewer and the axial direction. The two white dash lines in Fig. 2b are edges of the $25\ \mathrm{cm} \times 25\ \mathrm{cm}$ hole in the aluminum support. Flame beyond the two lines are extended flames along the support. In this case, as the oxygen concentration is slightly reduced below the ambient concentration, small flame holes flash while this size holes are not sufficient to destabilize the blanket flame, and they can always ‘healing’ over time. Only when the oxygen concentration further decreases at 17.23 %, larger size hole can terminate the one-dimensional blanket flame. The hole may move, but can’t be healed. This phenomenon can be characterized by a decreased *Da*, which varies along the flame sheet as the oxygen concentration decreases. Holes develop in the flame sheet below a threshold *Da*. Further decreasing the oxygen concentration causes the hole to become larger and splitting into multiple holes. Eventually, at $X_{O_2} = 12.59\%$, the holes expand to cover a large area, increasing the flame instability up to the point of total extinction. Based on the transformation of the flame, the event triggering the extinction appears to be the development of these holes. Here, we define two extinction modes: 1) local extinction which occurs at the incipient unhealable moving flame hole terminating the one-dimensional blanket flames, and 2) total extinction which is associated with the lowest oxygen concentration limits. The behavior is also seen in other cases.

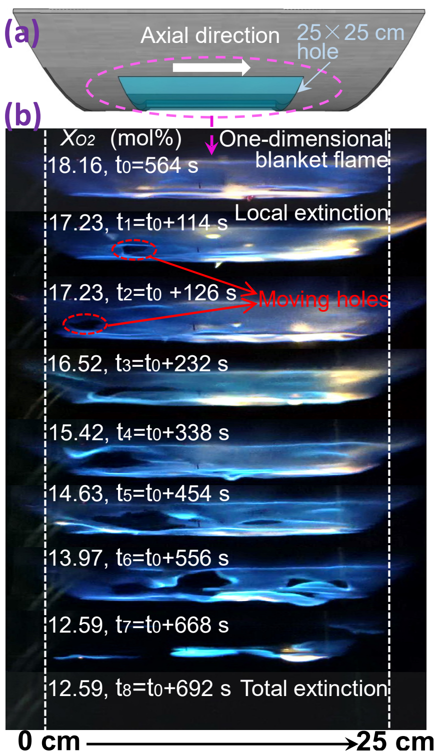

Fig. 2. (a) A diagram of low inclined viewer; (b) Sequential flame images from local to total extinction with reduced oxygen concentration from lower inclined view of Camera 1 (*R* = 100 cm, ice bath).

Flammability boundary of varied stretch rates

Figure 3 shows the extinction boundary from local to total at reduced oxygen concentrations of varied stretch rates, where the stretch rate is calculated based on (Eq. 2-4), where T^* in (Eq. 2) is selected as an average value between the flame temperature and pyrolysis temperature, assumed to be invariant at about 900 K [6]. The calculated stretch rates in this experiment are at the range of 1.8~18 s^{-1} corresponding to radii of 200~2.5 cm. It can be seen that the local extinction separates the regions of the stable and unstable, while the total extinction is the lowest limit of the unstable region.

The phenomenon of this critical state can also be characterized by *Da*. In actual flames, at a fixed stretch rate, when *Da* becomes small and approaches the Extinction Damkohler Number (Da_E), the characteristic flow time becomes too small as compared to the chemical reaction time and hence flame extinguishes. When *Da* is larger, the inherent heat losses can reduce the maximum flame temperature, and consequently, induces flame extinction. Thus, both small and large *Da* can result in flame extinction. As stretch rate is often incorporated into *Da* and they are inversely proportional, both high and low stretch rate can also lead to extinction. It is obvious that two kinds of Da_E establish at low and high stretch rate: one is the radiative extinction $Da_{E,R}$ at low stretch rate and the other is kinematic extinction $Da_{E,K}$ at high stretch rate [7]. With the increasing stretch rate, both $Da_{E,R}$ and $Da_{E,K}$ decrease. The theory is consistent with the experimental results that at a fixed oxygen concentration, extinction occurs at two different stretch rates: one is at high stretch rate and the other is at low stretch rate in Fig. 3. Stretch rates between the two extinction values are flammable stretch rates.

As the oxygen concentration decreases, the flammable stretch rates narrow down, and eventually merge at one point. When the oxygen concentration decreases below the merging point of local extinction, a steady stagnation-point diffusion flame cannot be established regardless of the values of stretch rate. Likewise, when the oxygen concentration is below the merging point of total extinction, there is no flame exist. Hence both local and total extinction have a 'U'-shape flammability map: quenching associated with lower stretch rates (<10 s^{-1}) and blowoff associated with higher stretch rates (>10 s^{-1}), where 10 s^{-1} is the transition point reported by a previous study [4]. That's to say, varied stretch rate is a good candidate for alternative fire suppressant, such as increasing flame stretch to "blowoff" according to enhancing forced flow velocity gradient over flame surface or reducing the sample radius of curvature, and decreasing flame stretch to "quenching" by increasing sample radius. Furthermore, reduced oxygen concentration is beneficial to narrow the flammable stretch rates.

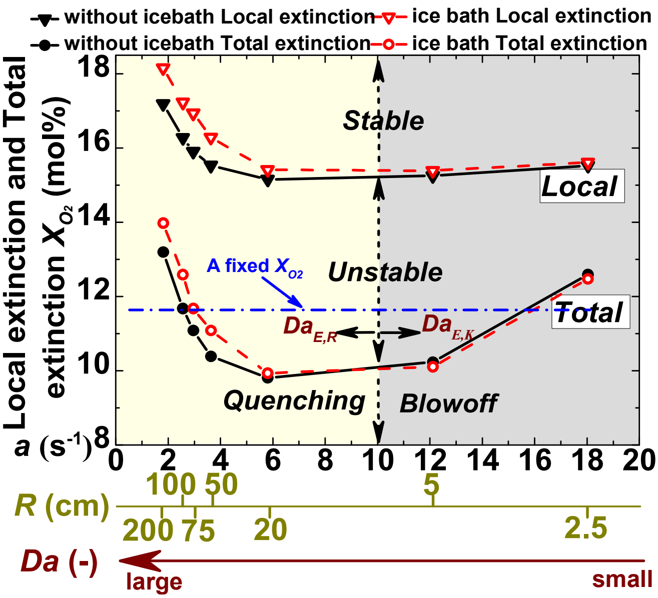

Fig. 3. Flammability boundary of varied stretch rates.

One more thing should be noticed is that extinction at low stretch rate is influenced by heat loss and corresponds to "quenching" which is very similar to flame extinction happened in microgravity environment due to excessive heat loss. Therefore, low stretch rate plays an important role in microgravity flames, in other words, extinction of microgravity flames can be simulated in a terrestrial environment by low stretched flames.

Effect of heat loss due to ice bath

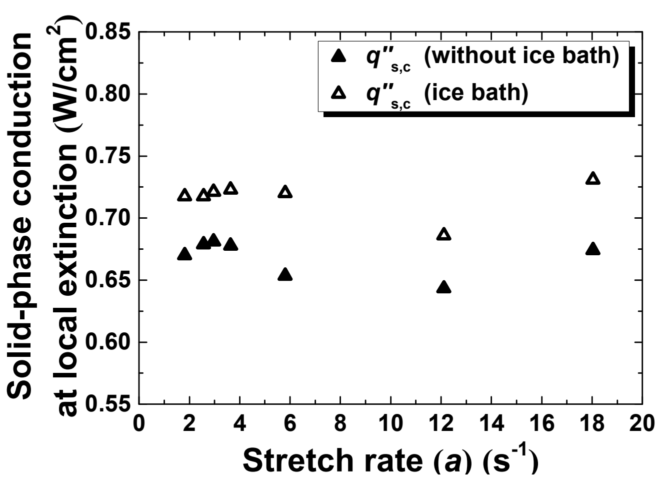

Fig. 4. Solid-phase conduction at local extinction versus stretch rate.

In order to further understand the effect of heat loss upon extinction, ice bath was employed covering the upper surface of the curved PMMA to increase the solid in-depth conduction. The comparative analysis of cases with and without ice bath shows that ice bath increases the solid heat loss according to enlarging the solid-phase conduction for both lower and higher stretch rates as show in Fig. 4.

Because quenching is controlled by heat transfer, ice bath makes extinction occurs more easily in quenching region at lower stretch rates from the flammability map (Fig. 3), while has little effect upon blowoff branch at higher stretch rates. This result has an implication for us that a quick way to quench the flame is to greatly enlarge the solid-phase heat loss such as putting dry ice on the back surface of fuels.

Conclusions

Equipment of obtaining a range of stretch rates including very high and low cases together with reduced oxygen concentration in a terrestrial environment precluding the influence of buoyancy was firstly realized. Analysis of stretch rate showed that there exhibits a dual extinction turning point behavior in that flame extinction occurs not only for sufficiently high stretch rate and minimal radiative heat loss, but also for sufficiently low stretch rate and extensive heat loss. This study is instructive for extinction of fires. Detailed conclusions are as follows:

(1) Holes in the flame sheet triggered extinction and can be characterized by *Da*. Local and total extinction modes were proposed to distinguish “Stable”, “Unstable” and “Extinction” regions of this stretched diffusion flames, and both local and total extinction modes have a ‘U’-shape flammability map versus stretch rate.

(2) Quenching is associated with radiative extinction $Da_{E,R}$ at low stretch rate which is similar to microgravity flame extinction due to extensive heat loss. While blowoff is connected with kinematic extinction $Da_{E,K}$ at high stretch rate and commonly seen in highly forced flow environment. Varied stretch rate is a good candidate for alternative fire suppressant, such as increasing flame stretch to blowoff by enhancing flow velocity gradient or reducing the sample radius, and decreasing flame stretch to quenching by increasing sample radius. Furthermore, reduced oxygen concentration is beneficial to narrow the flammable stretch rates.

(3) Ice bath enlarges heat loss according to increasing the solid in-depth conduction. Extinction occurs more easily in quenching region with the presence of ice bath because quenching is controlled by heat transfer. While ice bath has little effect upon blowoff branch. It inspires us that a quick way to quench the flame is to greatly enlarge the solid-phase heat loss such as putting dry ice on the back surface of fuels.

Acknowledgements

This work was sponsored by the National Natural Science Foundation of China (No. 51636008, 51576186, 51323010), Key Research Program of the Chinese Academy of Sciences (No. QYZDB-SSW-JSC029), National Key R&D Program (No. 2016YFC0801500), Fundamental Research Funds for the Central Universities (No. WK2320000042).

References

[1] S.H. Chung, C.K. Law, An invariant derivation of flame stretch, Combustion and Flame 55(1) (1984) 123-125.

[2] B. Karlovitz, D.W. Denniston, D.H. Knapschaefer, F.E. Wells, Studies on turbulent flames, Symposium (International) on Combustion 4(1) (1953) 613-620.

[3] J.S. T'ien, M. Endo, Material flammability: A combustion science perspective, Procedia Engineering 62 (2013) 120-129.

[4] D.W. Foutch, J.S. T'ien, Extinction of a stagnation-point diffusion flame at reduced gravity, AIAA Journal 25(7) (1987) 972-976.

[5] M.C. Johnston, J.S. T'ien, Gravimetric measurement of solid and liquid fuel burning rate near and at the low oxygen extinction limit, Fire Safety Journal 91 (2017) 140-146.

[6] S.L. Olson, P.V. Ferkul, Microgravity flammability boundary for PMMA rods in axial stagnation flow: Experimental results and energy balance analyses, Combustion and Flame 180 (2017) 217-229.

[7] B.H. Chao, C.K. Law, Asymptotic theory of flame extinction with surface radiation, Combustion and Flame 92(1-2) (1993) 1-24.